Postnatal development of the rat cochlear nuclei. Qualitative study with the glial markers GFAP and vimentin

F.J. Valderrama-Canales[1] and P. Gil-Loyzaga[2]

1- Departamento de Anatomía y Embriología Humana I, Facultad de Medicina, Universidad Complutense de Madrid, 28040 Madrid, Spain

2- Departamento de Cirugía II, Facultad de Medicina, Universidad Complutense de Madrid, 28040 Madrid, Spain.

SUMMARY

The cochlear nuclei are the first central step in the ascending auditory pathway. Studies on the development of the cochlear nuclei have been devoted to the histogenesis, neuronal maturation and migration, development and setting up of projections, and development of neurotransmitters. During postnatal maturation of the cochlear nuclei, neurons migrate to their definitive positions and the connections of the nuclear complex are established and refined. However, in spite of the fundamental role of the glia during the morphogenesis of the central nervous system, little attention has been paid to the presence and function of the astroglial cells within the cochlear nuclei. In light of this, here we investigated the presence, morphology and temporal patterns of the appearance of the astroglial cells of the cochlear nuclei. To identify the glial cells, monoclonal antibodies were used to detect glial fibrillary acidic protein and vimentin. The immature intermediate filament cytoskeleton of astrocytes it is made up of vimentin, and that of radial glial cells, and, as development proceeds, glial fibrillary acidic protein constitutes the intermediate filament cytoskeleton in mature astrocytes.

Our study revealed the presence of radial glial cells and astrocytes within the cochlear nuclei along postnatal development. A reciprocal relationship in the distribution of glial fibrillary acidic protein and vimentin during maturation of the cochlear nuclear complex is reported.

The morphology, temporal patterns of appearance, and maturation of glial cells are discussed in relation to the morphogenesis and maturation of the cochlear nuclei, placing the possible role of radial glia in the migration of cochlear cells and in the guidance of the axons to their functional targets.

INTRODUCTION

The cochlear nuclei (CN) are the first central step in the ascending auditory pathway. The CN include two main regions called ventral cochlear nucleus (VCN) and dorsal cochlear nucleus (DCN) (Ramón y Cajal, 1909; Lorente de Nó, 1933, 1981). The VCN can be subdivided into an anterior ventral cochlear nucleus (AVCN) and a posterior ventral cochlear nucleus (PVCN) (Ramón y Cajal, 1909; Lorente de Nó, 1933, 1981). The DCN is a laminated structure composed of three principal layers: molecular, pyramidal, and the deep polymorphic region (Osen, 1969; Berrebi and Mugnaini, 1991). The cytoarchitectural features of the CN are completed by the cochlear granule cell domain (GCD), which comprises several areas of small neurons (Mugnaini et al., 1980ab). Developmental studies of the CN have principally been related to histogenesis (Taber Pierce, 1967; Altman and Bayer, 1980; Martin and Rickets, 1981), neuronal maturation and migration (Schwartz and Kane, 1977; Willard and Martin, 1986; Schweitzer, 1990;

López-Sánchez, 1993) and development of projections (Schweitzer and Cant, 1984, 1985; Angulo et al., 1990).

During the morphogenesis of the central nervous system a series of complex processes occurs in which interactions between neurons and glial cells are of decisive importance. Associations between migrating neurons and radial glial cells have been demonstrated in the cerebral cortex (Rakic, 1972) and cerebellum (Rakic, 1971; Hatten, 1990). Glial cells provide a favourable environment through which growing axons migrate (Joosten and Gribnau, 1989; Silver et al., 1993; Reese et al., 1994; Marcus and Mason, 1995) thus guiding axons and growth cones during the formation of neuronal circuits. Also, glial cells compose boundaries that surround functional groups of neurons and their projections, avoiding mismatching in neuronal connectivity or building compartments among different nerve territories (Laywell and Steindler, 1991; Steindler, 1993). Nevertheless, despite the prominent role of the glia during development, the presence and functional roles of the glial cells during the postnatal development of the CN have received little attention. Only the works of Rigss et al. (1995) and Burette et al. (1998) have addressed the presence and putative roles of glial cells during the postnatal development of the CN. The former paper (Riggs et al., 1995), focus at the postnatal development of glial fibrillary acidic protein (GFAP) structures within the hamster DCN, suggests that GFAP-immunoreactive structures could play an early role in establishing the tonotopic axis of the DCN. The latter (Burette et al., 1998) examines the changes in the patterns of GFAP and S100β along the postnatal development of the CN of the rat, and discusses a linked maturation between CN astrocytes and neurons. Regardless of the scope, species studied, and results of these papers, some discrepancies are apparent.

Taking into account the background to the topic, our work qualitatively examines the presence of structures immunoreactive to glial fibrillary acidic protein (GFAP) and vimentin (VIM) in order to study the presence, distribution, and putative roles of astroglial cells during the postnatal development of the CN of the rat. We selected these classical markers because it is well known that in immature astrocytes, as well as in radial glial cells, intermediate filaments consist of VIM (Dahl et al., 1981; Bignami et al., 1982; Lazarides, 1982; Cochard and Paulin, 1984; Pixley and De Vellis, 1984) and, as maturation proceeds, VIM disappears from astroglia and intermediate filaments consisting of GFAP appear (Levitt and Rakic, 1980; Schnitzer et al., 1981; Tapscott et al., 1981). It is also known that in the later deve-

lopmental stages, radial glial cells differentiate into astrocytes (Schmechel and Rakic, 1979; Voigt, 1989; Hunter and Hatten, 1995) and that this astrocyte maturation is accompanied by modifications of their intermediate filament composition. Thus, it is generally accepted that GFAP constitutes the intermediate filament cytoskeleton in mature astrocytes (Eng et al., 1971; Bignami et al., 1972; Eng, 1985).

MATERIALS AND METHODS

Animals and tissue preparation

A total of 29 Long-Evans rats, bred in our own colony, were used in this study. Rats at the following postnatal days (PND), PND 0 (n = 6), PND 3 (n = 5), PND 7 (n = 4), PND 9 (n = 6), PND 15 (n = 4), PND 21 (n = 4) were sacrificed by perfusion under deep chloral hydrate anaesthesia (300 mg/kg, i.p.), except neonates and PND 3, which were anesthetized by hypothermia. Animals from two different litters were used for each developmental stage.

It is well known that the composition of fixatives can affect the ability of antibodies against GFAP to recognize their corresponding epitopes (DeArmond and Eng, 1984; Eng and Lee, 1995), especially the use of aldehydes (Eng and Lee, 1995). Thus, in order to compare and discard any false results produced by the fixation procedure, we used two different protocols for the fixatives. The GFAP antibody of the G-A-5 clone affords the best results when the tissue was fixed with alcohol (Altmannsberger et al., 1982), although it has also been shown that some paraformaldehyde-based fixatives yield excellent results (Müller, 1992). Therefore, animals from PND 7 were perfused transcardially through the ascending aorta either with a mixture of 2% acetic acid in absolute ethanol (Valderrama-Canales et al., 1993) or with Zamboni's fixative (15% saturated aqueous picric acid, 4% paraformaldehyde solution in 0.1 M phosphate buffer). Brainstems were quickly removed from the skull and postfixed overnight in the same fixatives used in the perfusion. Ethanol-acetic-fixed brainstems were paraffin-embedded following the usual procedures, and the pieces were sectioned on the coronal plane at 8 µm. Zamboni-fixed brainstems were sectioned coronally at 50 µm on a vibratome (TPI series), collected in cold (4ºC) phosphate buffer saline (PBS) and washed carefully until the picric acid was completely removed.

Animals from PND 0 and PND 3 were decapitated, and the skull was immediately opened in either the ethanol mixture or Zamboni's fixative, and fixed by immersion for 6 hours. Then, brainstems were dissected out and placed in the fixative for 2 days and, after washing the excess

of picric acid, routinely embedded in paraffin or sectioned on a vibratome with no previous embedding, as detailed above.

Immunohistochemical procedures

All immunohistochemical incubations were performed at room temperature, unless otherwise stated. Before preincubations, endogenous peroxidase was blocked with 0.3% H_2O_2 in PBS for 20 minutes with gentle stirring, and rinsed thoroughly in PBS.

Free-floating vibratome sections were preincubated with 30% normal horse serum (NHS) and 0.5% Triton X-100 (TX-100) in PBS for 30 minutes. Without previous rinsing, sections were incubated either with monoclonal anti-GFAP (clone G-A-5, Boehringer Mannheim) or monoclonal anti-VIM (clone vim-9, Boehringer Mannheim) diluted 1:4 in PBS solution containing 10% NHS, 1% bovine serum albumin (BSA), 5% sucrose and 0.5% TX-100. After 2-3 days of incubation at 4ºC with gentle shaking, sections were rinsed in PBS and further incubated for two hours with a horse biotinylated anti-mouse IgG (Vectastain, Vector) diluted 1:200 in PBS, and developed according to the ABC-peroxidase technique (Vectastain, Vector) using 0.01% of H_2O_2 plus 0.7 mg/ml 3.3´-diaminobenzidine (DAB; Sigma) in Tris buffer saline (0.05 M, pH 7.60). Sections were mounted onto poly-L-lysine-covered glass slides, air dried, dehydrated, and coverslipped with eukitt.

The paraplast-embedded sections were deparaffinized, rehydrated, washed in PBS, and preincubated (30 minutes) with 30% NHS in PBS with 0.1% TX-100. Incubations were performed over 14-16 hours either with the anti-GFAP or the anti-VIM (1:4 in PBS with 1% BSA, 30% NHS, and 0.1% TX-100). After rinsing in PBS, sections were incubated with the biotinylated monoclonal secondary antibody (anti-mouse IgG made in horse; Vectastain, Vector) at a dilution of 1:200 in PBS (2 hours). Finally, sections were processed with the ABC-peroxidase system (Vectastain, Vector) and developed with DAB as chromogen, as described for the vibratome sections. Sections were dehydrated and slide-mounted with eukitt.

Controls

Negative controls were performed by replacing the primary antibody by the corresponding normal serum during the first incubations. No labelling was observed in any control section. Positive controls were carried out on cerebellar sections and specific glial immunoreactivity was observed (not shown). All sections were observed and photographed with a Leica DRMB photomicroscope.

RESULTS

For PND 0 brainstems, identification of the tissue sections that comprised the cochlear nuclei (dorsal and ventral) was made following the atlas of Paxinos et al. (1991).

General observations

The results obtained show a conspicuous specific immunoreaction along all the ages studied. For both GFAP and VIM, the use of Zamboni- or alcoholic-fixed tissue did not reveal differences in the overall results of the immunoreaction. However, the sectioning techniques gave dissimilar features in the final histological results. Thus, for PND 0, PND 3, and PND 7 the quality of the vibratome sections was not good enough to preserve the morphology of the CN, in contrast with the well preserved characteristics of the classic paraffin-embedded tissues. On the other hand, the vibratome sections allowed the observation of the complete morphology of immunoreactive structures, providing a more accurate image of the astroglial cytoarchitecture of the CN.

Along the period studied, the immunohistochemical results revealed a reciprocal relationship in the distribution of GFAP and VIM during the maturation of the CN. VIM-immunoreactive elements became less common from PND 0 to PND 21, whereas GFAP-immunoreactive structures increased along the same time interval. VIM immunoreactivity (VIM-ir) was present from PND 0 and remained robust on PND 7, but decreased strikingly from PND 9 onwards and was evident only in a few specific regions on PND 21. In contrast, GFAP immunoreactivity (GFAP-ir) was scarce along the first postnatal week but increased from PND 9 to PND 21.

In addition, GFAP-ir and VIM-ir had dissimilar patterns in several tissues. Thus, the pia mater, the choroid plexus, and the vascular endothelium were always immunoreactive to the VIM antibody, whereas they were always negative for GFAP immunostaining. Ependymocytes showed dissimilar patterns of immunostaining: from PND 7 onwards ependymal cells were consistently immunopositive for VIM but, before this period, they seemed to exhibit a gradient in their immunoreactivity. Hence, within the VCN on PND 0 and PND 3 ependymal cells are scattered and faintly VIM-ir, whereas in the DCN there were greater number of strongly VIM-ir ependymocytes. Regarding GFAP-ir, the ependymal cells became immunopositive as of PND 7, although some cells always remained immunonegative.

Postnatal day 0

At birth, both GFAP-ir and VIM-ir processes could be seen radiating from the pial and ventricular surfaces of the CN (Figs. 1, 2, 3). At the secondary rhombic lip (Taber Pierce, 1967) immu-
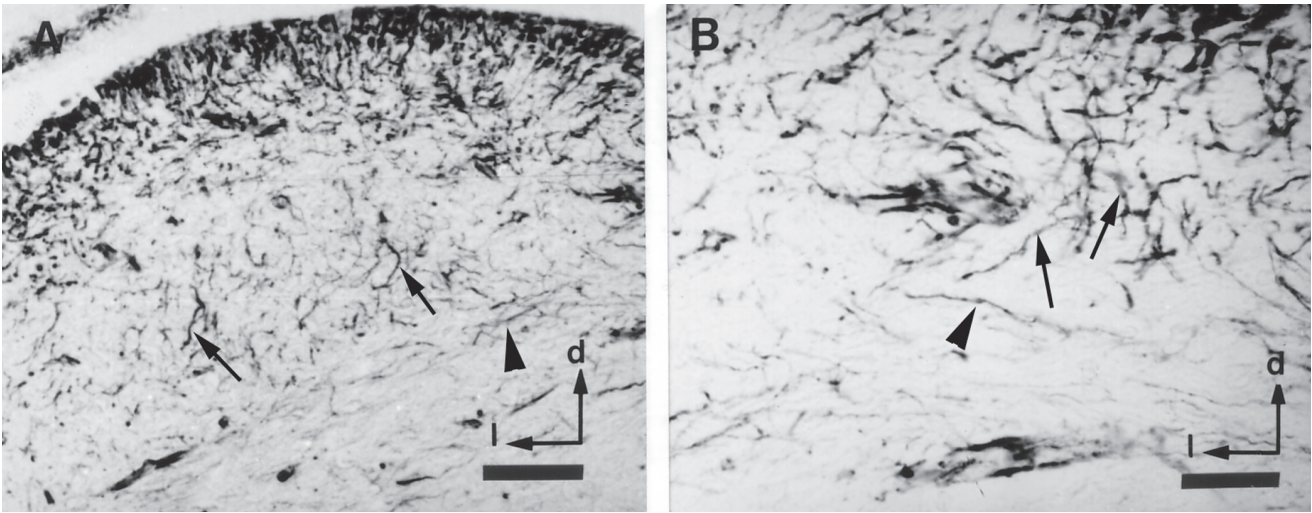
Fig. 1.- Coronal section of the rat DCN on PND 0. Vimentin-immunostained paraffin-embedded tissue. **A**: General view of the DCN. **B**: Magnification of A. Arrows: trans-strial fibres. Arrowheads: strially oriented fibres. Bar: 50 µm (A), 25 µm (B). d: dorsal. l: lateral.

noreactive radial glial cells spanned the subpial and subependymal surfaces. Within the DCN, the radial fibres arising from the subependymal surface crossed the putative molecular layer towards the deep polymorphic region (Figs. 1A, 1B, 3A, 3B). These fibres were arranged in a regular pattern called the trans-strial plane (Blackstad et al., 1984; Riggs et al., 1995) (Figs. 1A, 1B, 3A, 3B).

Within the deep nucleus, the VIM-ir processes appeared less organized but trans-strial fibres could be followed through the nucleus (Figs. 1A, 1B). Intercalated between the prospective molecular layer and the deep nucleus, there was a population of cross-sectioned VIM-ir fibres (Fig. 1A). At the medial limit of the DCN strially oriented VIM-ir fibres appeared (Fig. 1A, 1B), i.e., perpendicular to those trans-strially oriented (Blackstad et al., 1984). The VCN had fewer VIM-ir structures than the DCN (Figs. 2A, 2B). Nevertheless, some VIM-ir radial fibres ran from the ependymal layer to the core of the nucleus and some cross-sectioned fibres could be observed (Figs. 2A, 2B).

The immunostaining pattern of the anti-GFAP antibody partially reproduced that seen for the anti-VIM antibody, but with a smaller amount of immunopositive structures (Figs. 3A, 3B, 4A, 4B). In the ependymal cell layer, only some of the
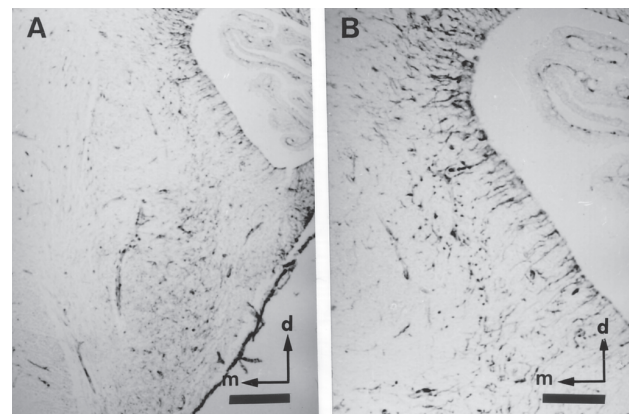

Fig. 2.- Coronal section of the rat VCN on PND 0. Vimentin-immunostained paraffin-embedded tissue. **A**: General view of the VCN. **B**: Magnification of A. Note the immunostained choroid plexus and pia mater. Bar: 100 µm (A), 50 µm (B). d: dorsal. m: medial.
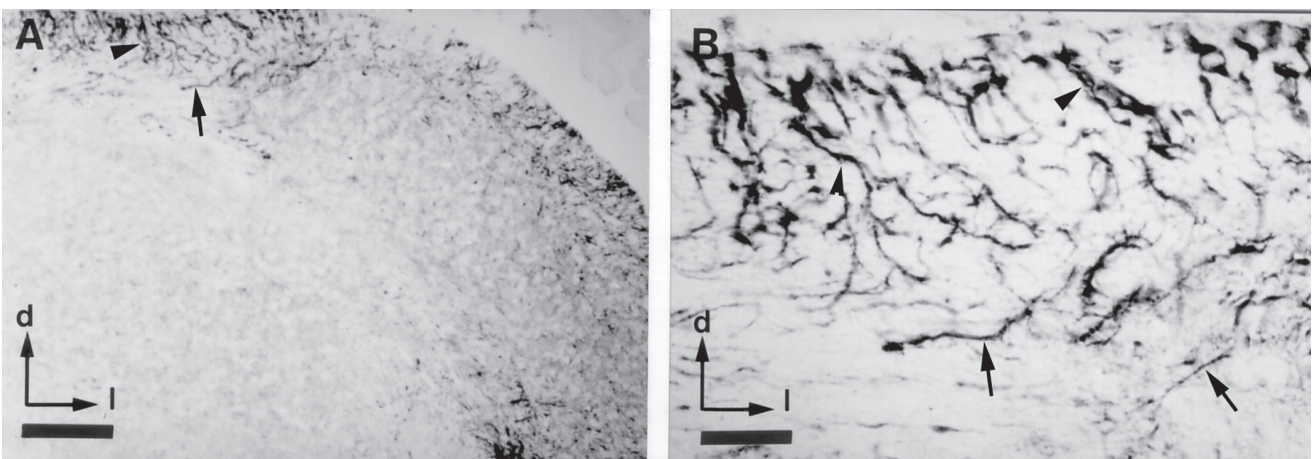

Fig. 3.- Coronal section of the rat DCN on PND 0. GFAP-immunostained paraffin-embedded tissue. **A**: General view of the DCN. **B**: Magnification of A. Arrowheads: trans-strial fibres. Arrows: strially oriented fibres. Bar: 50 µm (A), 25 µm (B). d: dorsal. l: lateral.

ependymal cells were GFAP-ir (Figs. 3B, 4B). The molecular layer of the DCN was crossed by GFAP-ir trans-strial fibres and at the medial extent of the nucleus some strial fibres limited the inferior cerebellar peduncle (Figs. 3A, 3B). The deep nucleus appeared almost completely devoid of GFAP-ir structures, except between the molecular layer and the deep nucleus, in the prospective pyramidal layer, where GFAP-ir fibres crossed the nucleus perpendicularly to the coronal plane (Fig. 3A). In the VCN, GFAP-ir processes were irregularly distributed and most of them were perpendicular to the section plane of the tissue (Figs. 4A, 4B).

Postnatal day 3

Within the DCN VIM-ir trans-strial fibres arose from cells located at the ventricular surface (Figs. 5A, 5B). Some fibres bent to assume a strial orientation at the level of the presumptive bor-

der between the molecular and the granular layers (Fig. 5B). The deep nucleus showed fewer of VIM-ir structures than the superficial layers, although strially-oriented fibres were present, mainly at the region of the dorsal acoustic stria (Fig. 5A). In the VCN, VIM-ir structures were scarce and less organized than in the DCN (Fig. 6). However, VIM-ir fibres were present at the rombic lip (Fig. 6A) and radiating from the ependymal layer (Fig. 6B).

The presence of GFAP-ir on PND 3 was still lower than that of VIM-ir (Figs. 7, 8). In the DCN, the distribution of GFAP-ir fibres resembled that seen on PND 0: trans-strial fibres crossed the superficial layers from the pial surface, and the deep nucleus was almost devoid of GFAP-ir (Figs. 7A, 7B). In the VCN, immunoreaction to the anti-GFAP antibody was rare (Fig. 8A), although some radial glial fibres could be seen arising from the ependymal layer (Fig. 8B).
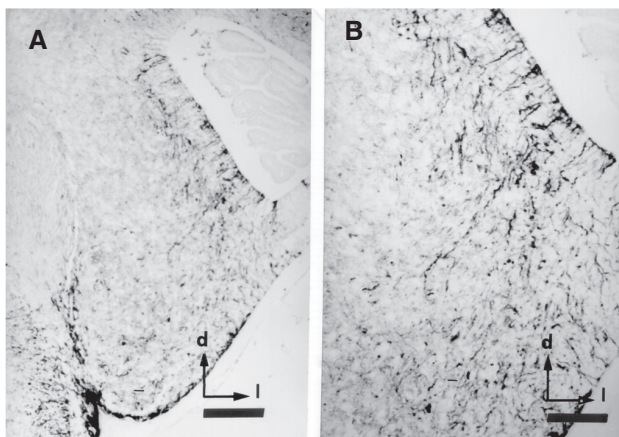

Fig. 4.- Coronal section of the rat VCN on PND 0. GFAP-immunostained paraffin-embedded tissue. **A**: General view of the VCN. **B**: Magnification of A. Note the choroid plexus devoid of immunostaining. Bar: 100 µm (A), 50 µm (B). d: dorsal. l: lateral.
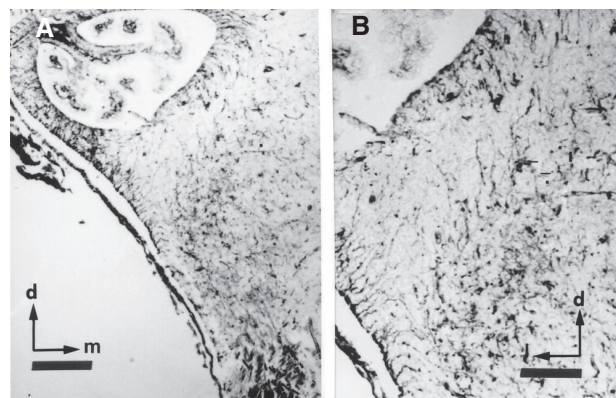

Fig. 6.- Coronal section of the rat VCN on PND 3. Vimentin-immunostained paraffin-embedded tissue. **A**: General view of the VCN. **B**: Magnification of A. Note the immunostained radial fibres, choroid plexus, and pia mater. Bar: 100 µm (A), 50 µm (B). d: dorsal. m: medial.
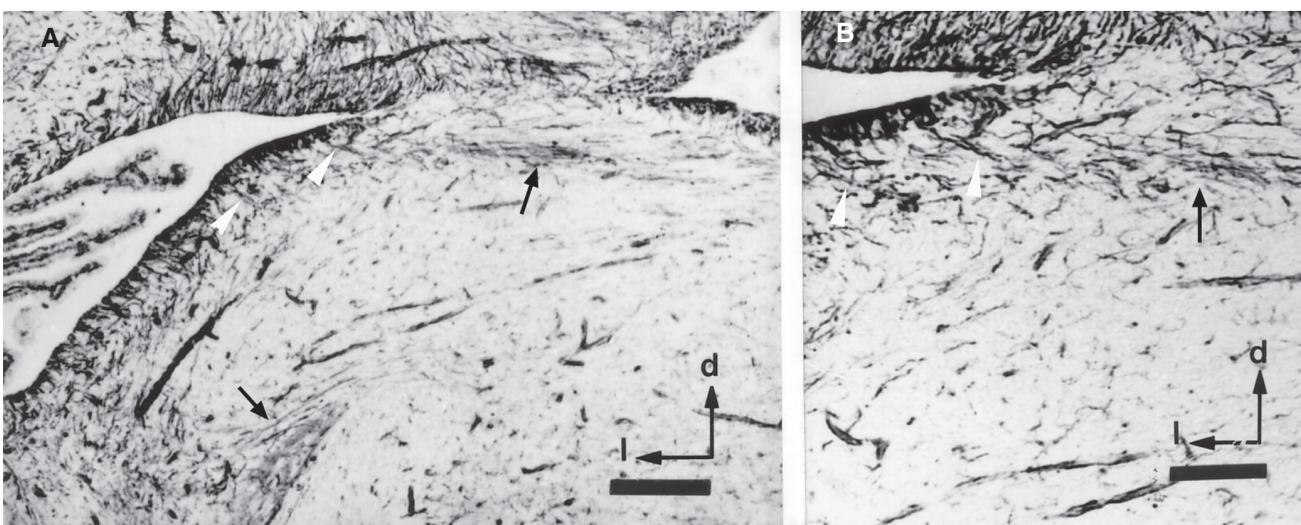

Fig. 5.- Coronal section of the rat DCN on PND 3. Vimentin-immunostained paraffin-embedded tissue. **A**: General view of the DCN. White arrowheads: trans-strial fibres. Arrows: strially oriented fibres. **B**: Magnification of A. Note the course of the fibres between the arrow and the arrowheads. Bar: 50 µm (A), 25 µm (B). d: dorsal. l: lateral.
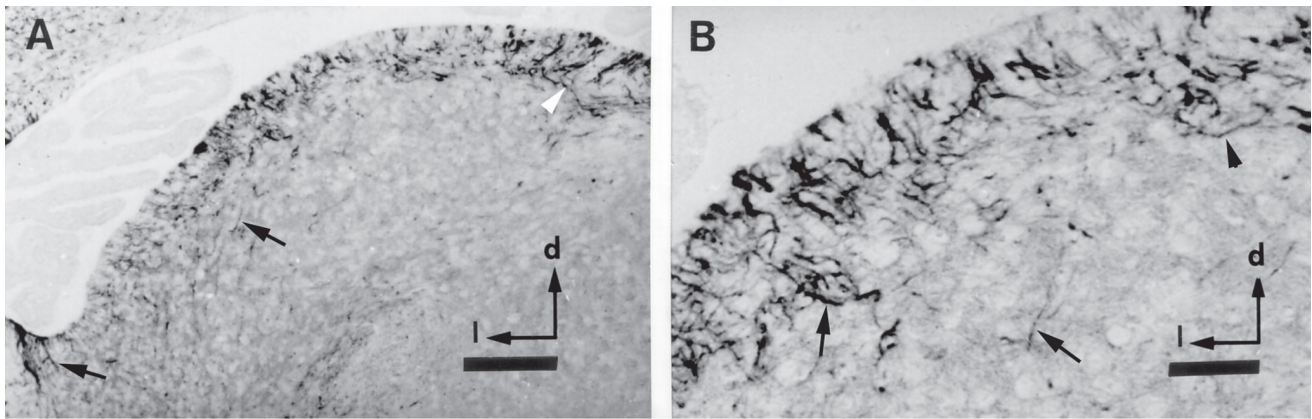
Fig. 7.- Coronal sections of the rat DCN on PND 3. GFAP-immunostained paraffin-embedded tissue. **A**: General view of the DCN. White arrowhead: strial fibres. Arrows: trans-strially oriented fibres. **B**: Detailed view of the DCN. Arrows: trans-strially oriented fibres. Arrowhead: strial fibres. Bar: 50 µm (A), 25 µm (B). d: dorsal. l: lateral.
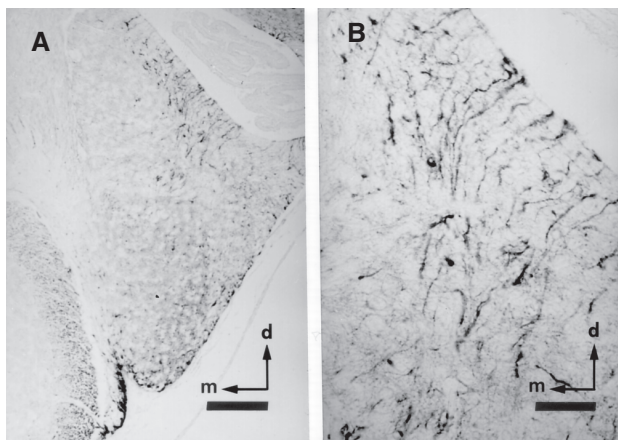

Fig. 8.- Coronal section of the rat VCN on PND 3. GFAP-immunostained paraffin-embedded tissue. **A**: General view of the VCN. **B**: Magnification of A. Immunostained radial fibres run from the ependymal layer. Bar: 100 µm (A), 50 µm (B). d: dorsal. m: medial.

Postnatal day 7

The density of VIM-ir structures was lower than in the preceding postnatal days, but the intensity of the immunostaining was comparable to that of the days before (Fig. 9). However, on PND 7 VIM-ir astrocytes were recognizable within the CN, mainly in the prospective GCD (Figs. 9B, 9E). In the DCN, some VIM-ir strial fibres were seen in the molecular layer (Figs. 9A, 9D). Within the VCN, the VIM-ir fibres were mainly found in the superficial granule cell layer (Figs. 9C, 9E).

Most ependymal cells in the CN had become GFAP-ir by PND 7 (Fig. 10). As occurred for the anti-VIM antibody, on PND 7 some astrocytes were labelled by the anti-GFAP antibody, also predominantly in the GCD (Figs. 10A, 10B, 10D). In the molecular layer of the DCN, some irregular fibres were observed (Fig. 10B). In the polymorphic layer, the GFAP-ir structures appeared as slightly immunostained puncta (Fig. 10B). The VCN showed irregularly oriented fibres, more abundant than in the preceding stages (Figs. 10C, 10D).

Postnatal day 9

For both the anti-VIM and the anti-GFAP antibodies, the immunostained structures, had changed by PND 9. The fibres had almost disappeared and the immunoreactive structures were mainly astrocytes (Figs. 11, 12).

The intensity of the VIM-immunostaining decreased dramatically on PND 9 and most VIM-ir astrocytes were only slightly immunostained (Figs. 11A, 11C). However, associated with several regions of the GCD, especially at the junction of the lamina with the superficial layer and in the subpeduncular corner, strong VIM-ir astrocytes were visualized (Figs. 11B, 11C). In the subpeduncular corner, sparse VIM-ir fibres were present.
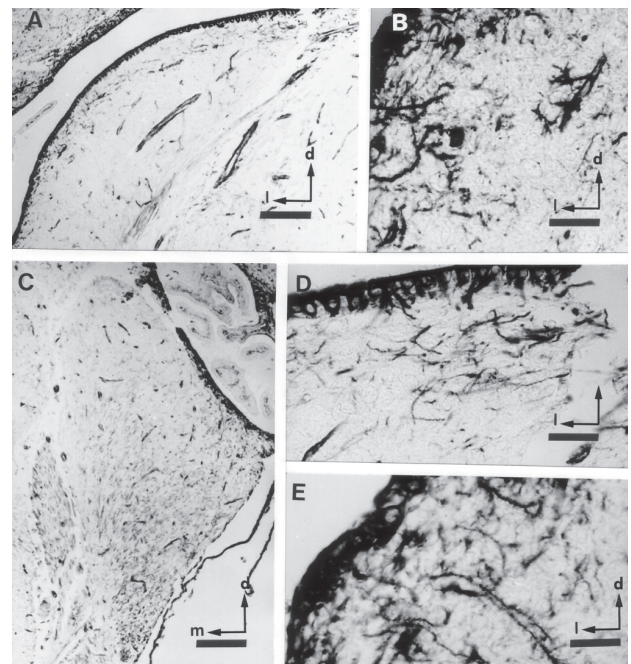

Fig. 9.- Coronal sections of the rat CN on PND 7. Vimentin-immunostained paraffin-embedded tissue. **A**: General view of the DCN. **B**, **D**: Detailed view of the DCN. Note the immunostained fibres and astrocytes. All the ependymocytes are immunopositive. **C**: General view of the VCN. **E**: Detailed view of the VCN. Note the immunostained fibres and astrocytes. All the ependymocytes are immunopositive. Bar: 100 µm (A, C), 25 µm (B, D), 20 µm (E). d: dorsal. m: medial. l: lateral.
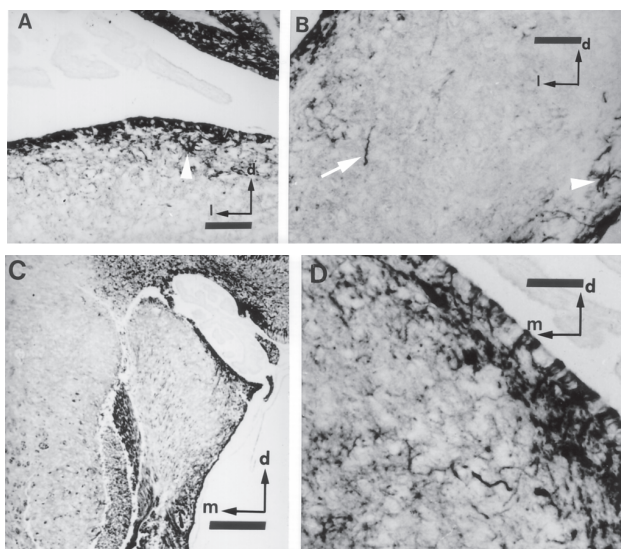
Fig. 10.- Coronal sections of the rat CN on PND 7. GFAP-immunostained paraffin-embedded tissue. **A**, **B**: Views of the DCN. Some scattered astrocytes (arrowheads) and fibres (arrow) can be seen. **C**, **D**: Views of the VCN. Most ependymocytes are immunopositive. The choroid plexus is immunonegative. Bar: 50 µm (A), 40 µm (B, D), 200 µm (C). d: dorsal. m: medial. l: lateral.

Fig. 11.- Coronal sections of the rat CN on PND 9. Vimentin-immunostained vibratome tissue sections. **A**: Border between the DCN and the PVCN. **B**: Astrocytes in the granule cell layer. **C**: View of the VCN. **D**: Astrocytes of the subpeduncular corner of the granule cell layer. Bar: 100 µm (A,C), 50 µm (B, D). d: dorsal. m: medial. l: lateral.

The presence of GFAP-ir structures and the intensity of immunolabelling were more important than those found for the VIM-ir structures at this stage (Fig. 12). For the first time during the postnatal days studied, all the ependymal cells were strongly GFAP-immunostained. Throughout the CN, GFAP-ir was not homogeneous and it was possible to identify GFAP-ir astrocytes with different degrees of staining (Figs. 12A, 12C). The GFAP-ir elements were mainly astrocytes although some short fibres that did not belong to any recognizable astrocyte somata could be observed (Figs. 12B, 12D). The largest population of GFAP-ir astrocytes within the DCN was seen in the molecular layer, whereas the structures of the deep nucleus showed the weakest immunostaining, despite some small clusters of strong GFAP-ir astrocytes located in it (Figs. 12A, 12B). The border between the DCN and the inferior cerebellar peduncle was clearly outlined by GFAP-ir strially-oriented astrocytes and their processes (Fig. 12A). Within the VCN, the superficial layer of granule cells and the subpeduncular corner included populations of strongly GFAP-ir astrocytes (Fig. 12C). Other territories of the VCN exhibited lower GFAP-immunostaining, although some clusters of highly GFAP-ir astrocytes were irregularly distributed within the nucleus (Figs. 12C, 12D).

Postnatal day 15

On PND 15, the ependymal cells and the endothelial cells of the blood vessels were strongly stained by the anti-VIM antibody. Within the DCN, scattered fibres and some astrocyte VIM-ir could be observed, mainly beneath the ependymal sur-
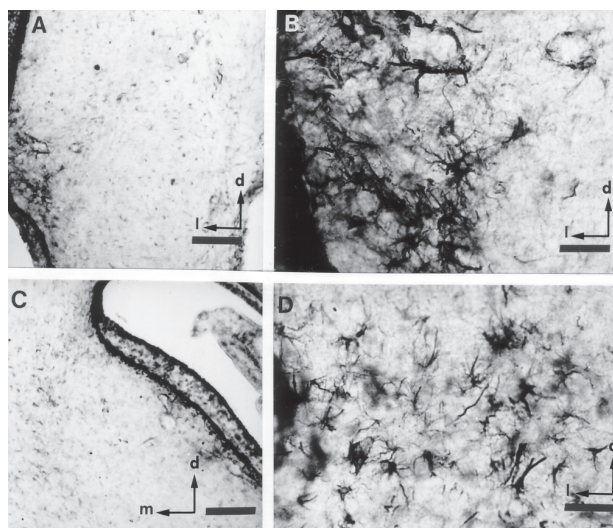
face, while in the VCN the subpeduncular corner and the superficial layer of granule cells displayed the highest density of VIM-ir astrocytes (Fig. 13).

The GFAP-ir astrocytes were numerous and strongly immunostained within the CN on PND 15, but their distribution was uneven (Fig. 14). The DCN showed a laminar distribution, with prominent GFAP-ir astrocytes occupying the molecular and granular layers and the medial lamina of granule cells (Figs. 14A, 14B). The deep nucleus also contained GFAP-ir astrocytes but only weakly
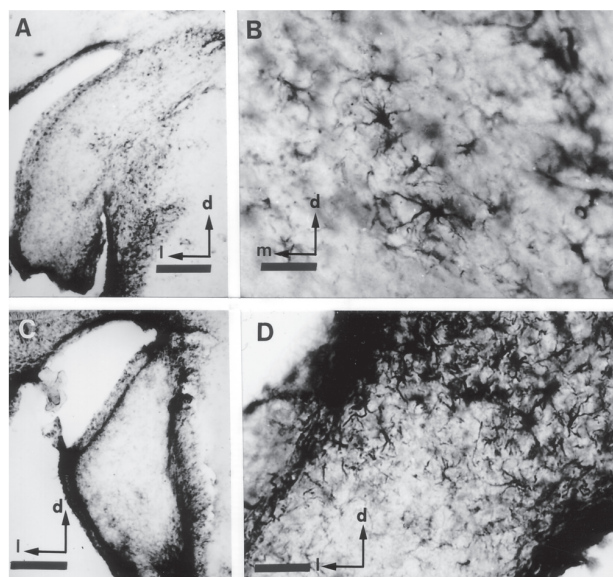

Fig. 12.- Coronal sections of the rat CN on PND 9. GFAP-immunostained vibratome tissue sections. **A**: General view of the DCN and the PVCN. **B**: Astrocytes of the deep nucleus. **C**: General view of the AVCN. **D**: Astrocytes of the subpeduncular corner of the granule cell layer. Bar: 200 µm (A,C), 20 µm (B), 40 µm (D). d: dorsal. m: medial. l: lateral.

immunostained (Fig. 14A). The prospective area of the lamina of granule cells, between the DCN and the PVCN, is apparent for its striking population of intense GFAP-ir astrocytes (Fig. 14B). The astrocytes of the VCN exhibited less GFAP-ir than those of the DCN (Figs. 14C, 14D). However, the AVCN was outlined by a boundary of strong GFAP-ir astrocytes (Fig. 14C). That boundary was constituted by GFAP-ir astrocytes located in the prospective areas of the subpeduncular corner of granule cells, dorsally (Fig. 14D); the superficial layer of granule cells, laterally; and the auditory nerve root, ventrally. The medial limit was demarcated by astrocytes belonging to the medial lamina of granule cells (Fig. 14D), the trapezoid body, and the vestibular nerve root.
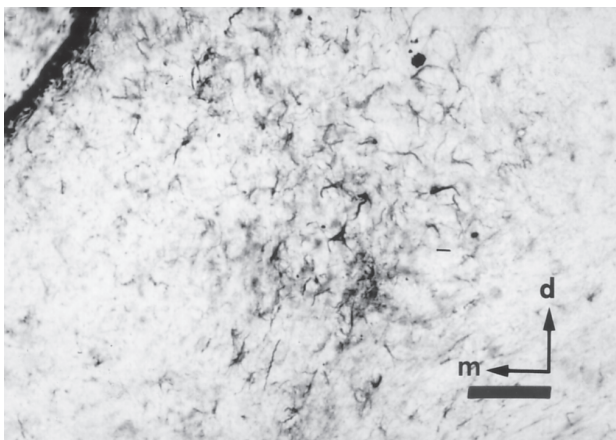

Fig. 13.- Coronal section of the rat AVCN on PND 15. Vimentin-immunostained vibratome tissue sections. Astrocytes of the subpeduncular corner of the granule cell layer. Bar: 50 µm. d: dorsal. m: medial.
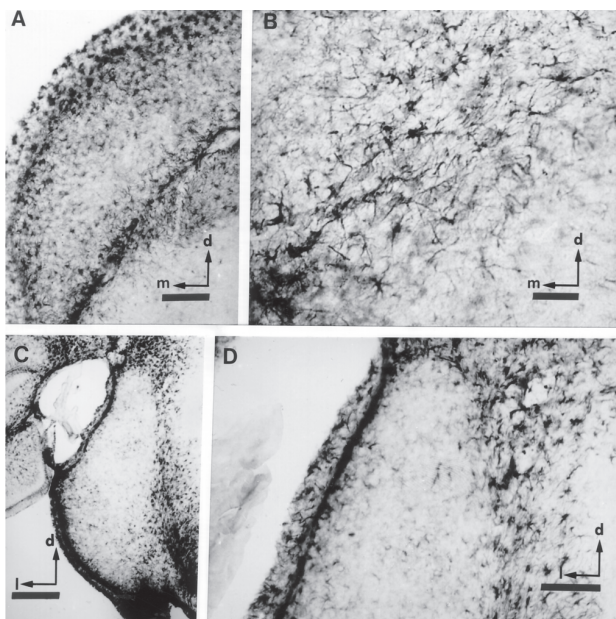

Fig. 14.- Coronal sections of the rat CN on PND 15. GFAP-immunostained vibratome tissue sections. **A**: General view of the DCN. **B**: Astrocytes of the granule cell layer. **C**: General view of the AVCN. **D**: Astrocytes of the subpeduncular corner and the medial lamina of the granule cell layer. Bar: 100 µm (A, D), 40 µm (B), 200 µm (C). d: dorsal. m: medial. l: lateral.

Postnatal day 21

The VIM-ir structures were limited to ependymal cells, vessels, and meninges.

On PND 21, the GFAP-ir had attained an adult-like pattern (Valderrama-Canales et al., 1993) (Fig. 15). GFAP-ir astrocytes displayed the typical star-shaped morphology (Fig. 15D) and the CN showed an outstanding degree of immunoreactivity, especially the molecular layer of the DCN (Fig. 15A) and the GCD (Figs. 15B, 15C).
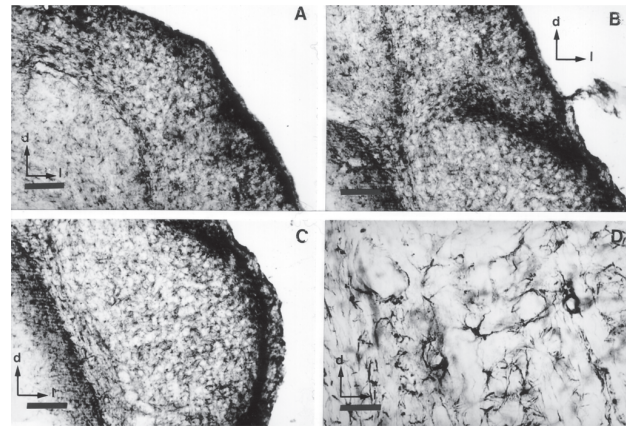

Fig. 15.- Coronal sections of the rat CN on PND 21. GFAP-immunostained vibratome tissue sections. **A**: View of the DCN. The molecular and pyramidal layers (outer layers) are strongly immunoreactive. The deep nucleus shows a lower density of immunostaining. **B**: View of the granule cell layer interposed between the DCN and the PVCN. The immunoreaction is particularly intense. **C**: View of the AVCN. The granule cell layer displays the most prominent immunostaining. **D**: Astrocytes of the descending branch of the primary afferents in the PVCN. Bar: 100 µm (A, B, C), 25 µm (D). d: dorsal. l: lateral.

DISCUSSION

Temporal and cellular patterns of expression of GFAP and VIM

Our immunohistochemical results point to a relationship in the distribution of VIM and GFAP during the maturation of the rat CN. At different stages, both GFAP and VIM antibodies labelled radial structures and/or astrocytes, but the anti-VIM antibody labelled more radial fibres while the anti-GFAP antibody labelled more astroglial cells. These data are consistent with the fact that processes and radial fibres are the most abundant immunostained structures from birth to PND 7 and from PND 9 onwards are replaced by immunoreactive astrocytes. In the opossum a reciprocal relationship in the changes of the immunoreaction of the two proteins along postnatal development has also been demonstrated (Elmquist et al., 1994). Regarding other cells and structures, our results agree with the development of the immunoreaction of the external glial membrane and the ependymal layer determined early on in the rat (Bignami and Dahl, 1974).

The differential expression of GFAP and VIM along the maturation of the CN could be due to cytoeskeletal changes in the astroglial cells, fact with strong experimental support. Thus, in the later developmental stages radial glial cells differentiate into astrocytes (Schmechel and Rakic, 1979; Voigt, 1989; Hunter and Hatten, 1995) and astrocyte maturation is accompanied by a modification of the intermediate filament composition of the cytoskeleton. In immature astrocytes intermediate filaments consist of VIM (Dahl et al., 1981; Bignami et al., 1982; Lazarides, 1982; Cochard and Paulin, 1984; Pixley and De Vellis, 1984) but as maturation proceeds VIM disappears from astrocytes and intermediate filaments consisting of GFAP appear (Levitt and Rakic, 1980; Schnitzer et al., 1981; Tapscott et al 1981) to constitute the mature intermediate filament cytoskeleton (Eng et al., 1971; Bignami et al., 1972; Eng, 1985).

Our results can be partially compared with previous findings. In the DCN of the hamster (Riggs et al., 1995) studies have focused on the appearance of structures immunoreactive to GFAP. In the rat CN, the presence of GFAP and S100β has been reviewed (Burette et al., 1998). In comparison with the development of GFAP-ir in the hamster DCN, our results in the rat DCN point to a more mature condition. This temporal lag of three days between the more immature hamster and the rat has been reported as a regular pattern of morphogenesis of the cochlear nuclear complex (Scheweitzer and Cant, 1984; Angulo et al., 1990). However, our observations of GFAP distribution and temporal patterns, together with those of Riggs et al. (1995), seem to contradict those of Burette et al. (1998), describing the developmental profile of GFAP in the rat DCN. More precisely, only on PND 5 did they observe some weakly GFAP-ir radial process in the DCN. Our results demonstrate the presence of GFAP-ir radial processes from the day of birth onwards. It is true that during this period VIM-ir radial processes are more numerous within the DCN, as explained above; nevertheless GFAP-ir radial fibres are also present. The difference between species, hamster and rat, and the use of a polyclonal antibody, raising a possible cross-reaction with vimentin, have been claimed to explain the divergence of observations (Burette et al., 1998). Our work discards both possibilities, since it was carried out on the rat and employed a GFAP monoclonal antibody. Hence, the discrepancy with the results of Burette et al. (1998) could be due to the use of a paraformaldehyde fixative for the demonstration of GFAP, as reported previously (DeArmond and Eng, 1984; Eng and Lee, 1995), especially when using the antibody of the G-A-5 clone (Altmannsberger et al., 1982).

In the rat, the compound action potentials of the cochlear nerve, the first physiological activity recorded in the auditory pathway, take place over 11-12 postnatally days (Carlier et al., 1979; Uziel et al., 1981). However, in the same species all of the cochlear functional parameters do not start before PND 15: the tuning curves mature along day 16-18 postnatally (Carlier et al., 1979), the thresholds and latencies of the compound action potential on PND 18 (Puel and Uziel, 1987), and the otoacoustic emissions between days 18 and 28 postnatally (Lenoir and Puel, 1987). Consequently, at least part of the astroglial population of the CN reaches a mature status by the time of the onset of hearing, since from PND 9 onwards astrocytes expressing GFAP are found, and most of them are adult-like during the period of the refinement of cochlear function. This developmental timing suggests that the onset and improvement of cochlear function occur when the astrocyte population of the CN has reached a certain status of maturity, as stated in other models (Müller, 1992, 1995).

Radial glia and axonal guide in the cochlear nuclei

Axon guidance by radial glial fibres has been clearly demonstrated (Joosten and Gribnau, 1989; Silver et al., 1993; Reese et al., 1994; Marcus and Mason, 1995) and within the CN previous works (Riggs et al., 1995) have suggested that the radial processes of the hamster DCN are functionally related to the guidance of the primary afferents to the DCN. In the rat, our results reveal radial fibres from PND 0 to at least PND 9. This presence could also be related to axonal guidance. However, in the rat the primary afferents are not good candidates as postnatal guidance elements, because they are present within the cochlear nuclear complex on the day of birth (Mattox et al., 1982; Neises et al., 1982; Angulo et al., 1990) and since the sixteenth gestational day (Angulo et al., 1990), as also occurs in the cat (Schwartz and Kane, 1977).

The best candidates as glial guidance elements are the axons of the parallel fibres of the granule cells. In the molecular layer of the DCN, the parallel fibres create a system with the dendritic spines of the pyramidal cells (Mugnaini et al., 1980b; Blackstad et al., 1984). It has been demonstrated that the spine formation of the pyramidal cells depends on the presence of such parallel fibres (Schweitzer and Cant, 1985; Schweitzer, 1990). This spine genesis occurs sequentially during the first two postnatal weeks (Schweitzer and Cant, 1985), concurrently with the presence of glial fibres in the molecular layer of the nucleus. Thus, both processes take place in the same area and with the same timing, and hence this morphogenetic sequence opens the possibility of a guide for the granule cells parallel fibres.

Radial glia and neuronal migration in the cochlear nuclei

The classic works of Rakic (1971, 1972) demonstrated that the granule cells of the cerebellum and the cerebral cortex migrate to their definitive positions by means of radial glial scaffolding. In addition, the similarity between the cerebellum and the DCN has been reported (Mugnaini and Morgan, 1987; Berrebi and Mugnaini, 1988) and it is well known that the cerebellar granule cells migrate onto the radial glia (Hatten and Mason, 1986; Hatten, 1990; Delaney et al., 1996). Cochlear granule cells generate in several waves until the second postnatal week (Altman and Das, 1966; Taber Pierce, 1967; Altman and Bayer, 1980), leaving the territories of genesis to occupy their definitive positions along PND 9 (López-Sánchez, 1993). The presence, at least until PND 9, of radial glial fibres in the GCD regions during the period of generation, reorganization and maturation of the cochlear granule cells provides a morphological substrate for cochlear granule cell migration. But not only cochlear granule cells are candidates to the migration process. Within the DCN, pyramidal and giant neurons are born at the same time (Schweitzer and Cant, 1985) and in the same proliferative area (Taber Pierce, 1967; Martin and Rickets, 1981). This area is different of that where the small neurons are born, located medial to the dorsomedial extent of the nucleus (Altman and Bayer, 1980; Willard and Martin, 1986). In the North American opossum it has been demonstrated that these large neurons of the DCN migrate postnatally (Willard and Martin, 1986), whereas in the rat (López-Sánchez, 1993) and in the hamster (Schweitzer and Cant, 1985) it has been shown that from an irregular mass located outside the nucleus the large neurons progressively gain a definitive mature position in the polymorphic layer. Our immunohistochemical images show a glial fibre arrangement fully comparable to the plan of neuronal migration reported by Willard and Martin (1986, figure 9). Thus, our morphological data support the feasibility of a neuronal migration process along the radial glial fibres of the DCN.

Acknowledgements

References

ALTMAN J and DAS G (1966). Autoradiographic and histological studies of postnatal histogenesis. II. A longitudinal investigation of kinetics, migration and transformation of cells incorporating thymidine in infant rats with special reference to postnatal neurogenesis in some brain regions. *J Comp Neurol*, 126: 337-390.

ALTMAN J and BAYER SA (1980). Development of the brainstem in the rat. III. Thymidine-radiographic study of the time of origin of neurons in the vestibular and auditory nuclei of the upper medulla. *J Comp Neurol*, 194: 877-904.

ALTMANNSBERGER M, WEBER K, HÖLSCHER A, SCHAUER A and OSBORN M (1982). Antibodies to intermediate filaments as diagnostic tools: human gastrointestinal carcinomas express prekeratin. *Lab Invest*, 46: 520-526.

ANGULO A, MERCHÁN JA and MERCHÁN MA (1990). Morphology of the rat cochlear primary afferents during prenatal development: a Cajal's reduced silver and rapid Golgi study. *J Anat*, 168: 241-255.

BERREBI AS and MUGNAINI E (1988). Effects of the murine mutation "nervous" on neurons in cerebellum and dorsal cochlear nucleus. *J Neurocytol*, 17: 465-484.

BERREBI AS and MUGNAINI E (1991). Distribution and targets of the cartwheel cell axon in the dorsal cochlear nucleus of the guinea pig. *Anat Embryol*, 183: 427-454.

BIGNAMI A and DAHL D (1974). Astrocyte-specific protein and neuroglial differentiation: an immunofluorescence study with antibodies to the glial fibrillary acidic protein. *J Comp Neurol*, 153: 27-38.

BIGNAMI A, ENG LF, DAHL D and UYEDA CT (1972). Localization of the glial fibrillary acidic protein in astrocytes by immunofluorescence. *Brain Res*, 43: 429-435.

BIGNAMI A, RAJU T and Dahl D (1982). Localization of vimentin, the nonspecific intermediate filament protein, in embryonal glia and early differentiating neurons. *Dev Biol*, 91: 286-295.

BLACKSTAD TW, OSEN KK and MUGNAINI E (1984). Pyramidal neurons of the dorsal cochlear nucleus: A Golgi and computer reconstruction study in cat. *Neuroscience*, 13: 827-854.

BURETTE A, JALENQUES I and ROMAND R (1998). Developmental distribution of astrocytic proteins in the rat cochlear nucleus. *Dev Brain Res*, 107: 179-189.

CARLIER E, LENOIR M and PUJOL R (1979). Development of cochlear frequency selectivity tested by compuound action potential tuning curves. *Hear Res*, 1: 197-201.

COCHARD P and Paulin D (1984). Initial expression of neurofilaments and VIM in the central and peripheral nervous system of the mouse embryo in vivo. *J Neurosci*, 4: 2080-2094.

DAHL D, RUEGER DC, BIGNAMI A, WEBER K and OSBORN M (1981). Vimentin, the 57.000 Dalton protein of fibroblast filaments, is the major cytoskeletal component in immature glia. *Eur J Cell Biol*, 24: 191-196.

DE ARMOND SJ and ENG LF (1984). Immunohistochemistry: techniques and application to neurooncology. In: Hamburger F (ed). *Progress in Experimental Tumor Research*, vol. 27. Karger, Basel, pp 92-117.

DELANEY CL, BRENNER M and MESSING A (1996). Conditional ablation of cerebellar astrocytes in postnatal transgenic mice. *J Neurosci*, 16: 6908-6918.

ELMQUIST JK, SWANSON JJ, SAKAGUCHI DS, ROSS LR and JACOBSON CD (1994). Developmental distribution of GFAP and vimentin in the Brazilian opossum brain. *J Comp Neurol*, 344: 283-296.

ENG LF, VANDERHAEGHEN JJ, BIGNAMI A and GERSTL B (1971). An acidic protein isolated from fibrous astrocytes. *Brain Res*, 28: 351-354.

ENG LF (1985). Glial fibrillary acidic protein: The major protein of glial intermediate filaments in differentiated astrocytes. *J Neuroimmunol*, 8: 203-214.

ENG LF and LEE Y (1995). Intermediate filaments in astrocytes. In: Kettenmann H, Ransom BR (eds). *Neuroglia*. Oxford University Press, Oxford, pp 650-670.

HATTEN ME (1990). Riding the glial monorail: a commom mechanism for glial-guided neuronal migration in different regions of the developing mammalian brain. *Trends Neurosci*, 13: 179-184.

HUNTER KE and HATTEN ME (1995). Radial glial cell transformation of astrocytes is bidirectional: regulation by a diffusible factor in embryonic forebrain. *Proc Natl Acad Sci USA*, 92: 2061-2065.

JOOSTEN EAJ and GRIBNAU AAM (1989). Astrocytes and guidance of outgrowing corticospinal tract axons in the rat. An immunocytochemical study using anti-vimentin and anti-glial fibrillary acidic protein. *Neuroscience*, 31: 439-452.

LAYWELL ED and STEINDLER DA (1991). Boundaries and wounds, glia and glycoconjugates. *Ann NY Acad Sci*, 633: 122-141.

LAZARIDES E (1982). Intermediate filaments: a chemically heterogeneous, developmentally regulated class of proteins. *Ann Rev Biochem*, 51: 219-250.

LENOIR M and PUEL JL (1987). Development of sf1-f2 otoacoustic emissions in the rat. *Hear Res*, 29: 265-271.

LEVITT P and RAKIC P (1980). Immunoperoxidase localization of glial fibrillary acidic protein in radial glial cells and astrocytes of the developing rhesus monkey brain. *J Comp Neurol*, 193: 815-840.

LÓPEZ-SÁNCHEZ JG (1993). *Maduración postnatal de los núcleos cocleares de la rata*. Tesis Doctoral. Universidad Complutense. Madrid.

LORENTE DE NÓ R (1933). Anatomy of the eighth nerve. III. General plan of structure of the primary cochlear nuclei. *Laryngoscope*, 43: 327-350.

LORENTE DE NÓ R (1981). *The Primary Acoustic Nuclei*. Raven Press, New York, pp 165-188.

MARCUS C and MASON CA (1995). The first retinal axon growth in the mouse optic chiasm: axon patterning and the cellular environment. *J Neurosci*, 15: 6389-6402.

MARTIN MR and RICKETS C (1981). Histogenesis of the cochlear nucleus of the mouse. *J Comp Neurol*, 197: 169-184.

MATTOX DE, NEISES G and GUILEY R (1982). A freeze-fracture study of the maturation of synapses in the anteroventral cochlear nucleus of the developing rat. *Anat Rec*, 204: 281-287.

MUGNAINI E and MORGAN JI (1987). The neuropeptide cerebellin is a marker for two similar neuronal circuits in rat brain. *Proc Natl Acad Sci USA*, 84: 8692-8696.

MUGNAINI E, WARR WB and OSEN KK (1980a). Distribution and light-microscopic features of granule cells in the cochlear nuclei of cat, rat, and mouse. *J Comp Neurol*, 191: 581-606.

MUGNAINI E, OSEN KK, DAHL A, FREIDICH VL and KORTE G (1980b). Fine structure of granule cells and related interneurons in the cochlear nuclear complex of cat, rat and mouse. *J Comp Neurol*, 191: 537-570.

MÜLLER CM (1992). Astrocytes in cat visual cortex studied by GFAP and S-100 immunocytochemistry during postnatal development. *J Comp Neurol*, 317: 309-323.

MÜLLER CM (1995). Glial cells and activity-dependent central nervous system plasticity. In: Kettenmann H, Ransom BR (eds). *Neuroglia*, Oxford University Press, Oxford, pp 805-814.

NEISES GR, MATTOX DE and GUILEY RL (1982). The maturation of the end bulb of Held in the rat anteroventral cochlear nucleus. *Anat Rec*, 204: 271-279.

OSEN KK (1969). Cytoarchitecture of the cochlear nuclei in the cat. *J Comp Neurol*, 136: 453-484.

PAXINOS G, TÖRK I, TECOTT LH, VALENTINO KL and FRITCHLE A (1991). *Atlas of the developing rat brain*. Academic Press, San Diego.

PIXLEY SKR and DE VELLIS J (1984). Transition between immature radial glia and mature astrocytes studied with a monoclonal antibody to vimentin. *Dev Brain Res*, 15: 201-209.

PUEL JL and UZIEL A (1987). Correlative development of cochlear action potential sensitivity, selectivity and frequency selectivity. *Dev Brain Res*, 37: 179-188.

RAKIC P (1971). Neuron-glia relationship during granule cell migration in developing cerebellar cortex: a Golgi and electron-microscopic study in *Macacus rhesus*. *J Comp Neurol*, 141: 283-312.

RAKIC P (1972). Mode of cell migration to the superficial layers of fetal monkey neocortex. *J Comp Neurol*, 145: 61-84.

RAMÓN Y CAJAL S (1909). *Histologie du Systeme Nerveux de l'Homme et des Vertébrés*. Maloine, Paris.

REESE BE, MAYNARD TM and HOCKING DR (1994). Glial domains and axonal reordering in the chiasmatic region of the developing ferret. *J Comp Neurol*, 349: 303-324.

RIGGS GH, COOPER NGF and SCHWEITZER L (1995). Patterns of GFAP-immunoreactivity parallel the tonotopic axis in the developing dorsal cochlear nucleus. *Hear Res*, 90: 89-96.

SCHMECHEL DE and RAKIC P (1979). A golgi study of radial glial cells in developing monkey telencephalon: morphogenesis and transformation into astrocytes. *Anat Embryol*, 156: 115-152.

SCHNITZER J, FRANKE WW and SCHACHNER M (1981). Immunocytochemical demonstration of vimentin in astrocytes and ependymal cells of developing and adult mouse nervous system. *J Cell Biol*, 90: 435-447.

SCHWARTZ AM and KANE ES (1977). Development of the octopus cell area in the cat ventral cochlear nucleus. *Am J Anat*, 148: 1-18.

SCHWEITZER L and CANT NB (1984). Development of the cochlear innervation of the dorsal cochlear nucleus of the hamster. *J Comp Neurol*, 225: 228-243.

SCHWEITZER L and CANT NB (1985). Development of oriented dendritic fields in the dorsal cochlear nucleus of the hamster. *Neuroscience*, 16: 969-978.

SCHWEITZER L (1990). Differentiation of apical, basal and mixed dendrites of fusiform cells in the cochlear nucleus. *Dev Brain Res*, 56: 19-27.

SILVER J, EDWARDS MA and LEVITT P (1993). Immunocytochemical demonstration of early appearing astroglial structures that form boundaries and pathways along axon tracts in the fetal brain. *J Comp Neurol*, 328: 415-436.

STEINDLER DA (1993). Glial boundaries in the developing nervous system. *Ann Rev Neurosci*, 16: 445-470.

TABER PIERCE E (1967). Histogenesis of the dorsal and ventral cochlear nuclei in the mouse. An autoradiographic study. *J Comp Neurol*, 131: 27-54.

131

Tapscott SJ, Bennet GS and Holtzer H (1981). Neuronal precursor cells in the chick neural tube express neuro-filament proteins. *Nature*, 292: 836-838.

Valderrama-Canales FJ, Gil-Loyzaga P, Merchán-Pérez A and López-Sánchez JG (1993). Astrocyte cytoarchitecture in the cochlear nuclei of the rat: an immunocytochemical study. *ORL*, 55: 313-316.

Voigt T (1989). Development of glial cells in the cerebral wall of ferrets: Direct tracing of their transformation from radial glia into astrocytes. *J Comp Neurol*, 289: 74-88.

Willard FH and Martin GF (1986). The development and migration of the cochlear large multipolar neurons in the North American opossum. *J Comp Neurol*, 248: 119-132.